Deformation and Failure of a Multi-wall Carbon Nanotube Yarn Composite

Thomas S. Gates[1]
Durability, Damage Tolerance and Reliability Branch, NASA Langley Research Center, Hampton, VA, 23681-2199, USA

Gail D. Jefferson[2]
Sarah-Jane V. Frankland[3]
National Institute of Aerospace, NASA Langley Research Center, Hampton, VA 23681-2199, USA

Abstract

Forests of multi-walled carbon nanotubes can be twisted and manipulated into continuous fibers or yarns that exhibit many of the characteristics of traditional textiles. Macro-scale analysis and test may provide strength and stiffness predictions for a composite composed of a polymer matrix and low-volume fraction yarns. However, due to the nano-scale of the carbon nanotubes, it is desirable to use atomistic calculations to consider tube-tube interactions and the influence of simulated twist on the effective friction coefficient. This paper reports laboratory test data on the mechanical response of a multi-walled, carbon nanotube yarn/polymer composite from both dynamic and quasi-static tensile tests. Macro-scale and nano-scale analysis methods are explored and used to define some of the key structure-property relationships. The measured influence of hot-wet aging on the tensile properties is also reported.

Background

A new form of carbon nanotube-based material has elicited interest for multifunctional applications such as strain sensing combined with structural reinforcement. This new form is grounded in the age-old ideas about spinning and the formation of small precursor materials into textile yarns (1), (2). Within the last 50 years, increasing emphasis has been placed upon analysis and test that provide insights on how various parameters, such as twist angle and fiber size, can influence mechanical properties of textiles. It is the objective of this paper to explore key structure-property relationships for a continuous, spun yarn, which uses multi-walled carbon nanotubes as the precursor material.

Recently, Baughman's group at University of Texas has developed a method for spinning carbon multi-wall nanotubes (MWCNTs) into a continuous yarn structure (3), (4). This process is amenable to standard textile manufacturing techniques and allows for variation in the number of strands, number of plies, and geometric factors such as twist and yarn diameter. Within the scope of this paper, we will consider mechanical testing of the yarn and explore models of the system

[1]Associate Fellow, Senior Researcher
[2]Postdoctoral Researcher
[3]Staff Scientist

from both atomistic and continuum relationships. Emphasis will be placed on descriptions of the elastic modulus and initial strength of this novel material system. Tests will also be performed to determine degradation from aging at hot/wet conditions.

Material System

The subject material tested at NASA Langley Research Center is a yarn-elastomer composite with a single layer of embedded, aligned, four-ply MWCNT yarn fibers. The precursor to the yarn structure is the MWCNT. The yarn material was supplied by Professor Ray Baughman, University of Texas at Dallas. The MWCNT yarn is created by simultaneously drawing and clockwise twisting (20 turns/mm) vertically aligned MWCNTs from a MWCNT forest to form a single yarn. Four of these singles are then twisted counterclockwise (4 turns/mm) forming a four-ply yarn (Figure 1). The MWCNT yarn is similar in many respects to standard textile materials (5), and can be viewed as a unique structure whose properties are dependent not only on the precursor material (MWCNTs) but on yarn geometry and manufacturing methods. To form the composite, five of the four-ply yarns were placed at approximately equal spacing along the length of the dog-bone shaped specimen (volume fraction~0.28%). The polymer used as the matrix material was a compliant elastomer that was cured in place along with the embedded yarns.

Figure 1. SEM micrograph of a longitudinal view of typical four-ply multi-wall carbon nanotube yarn (2500x; 15kV).

Analysis Models

In terms of length scales for the yarn structure under consideration, the following approximate structure-length relationships are assumed: MWCNT(10^{-9} m), fibers(10^{-7} m), single yarn(10^{-6} m), yarn plies(10^{-3} m). In this section of the paper, both atomistic and continuum mechanics approaches will be discussed. The intent is to provide an initial review of methods available to calculate critical parameters for prediction of stiffness and strength.

Generally, yarn twist is characterized by a twist multiplier (TM) (5).

$$TM = C^{1/2}\tau \tag{1}$$

where τ is the number of twists per unit length, and C is the linear density with units of mass per unit length. During tensile loading of the yarn, the apparent stress-strain behavior will generally have a short linear region characterized by slippage of the fibers followed by nonlinearity with considerable extension while the fibers continue to slip, and finally fiber failure occurs. During this axial loading of the yarn, off-angle forces in the yarn are generated by yarn twist.

Rao and Farris (6) considered the effects of material anisotropy on twisted yarns. They assumed that the yarn was composed of a series of thin-walled layers that resembles a unidirectional composite. The layers are located at a radial position (r) in a yarn of radius (R). The location of the filament is further defined by the angle (θ) between the single filament at r and the yarn major axis. Further, angle (θ) equals the angle (α) at maximum radius R. If one assumes low twist and $\alpha < 15^0$ then Rao arrives at an expression for the apparent Young's modulus of the yarn.

$$\hat{E} = E_z\left[\left(\frac{3T_o+1}{2dT_o}\right)+\frac{(1-d)^2}{d^3\tan^2\alpha}\ln\frac{(1-d)T_o+d}{T_o}\right]$$
$$d = \frac{E_z}{E_s}, \qquad T_o = \cos^2\alpha \tag{2}$$

The terms E_z and E_s are the longitudinal and shear modulus respectively of the fibers.

During yarn extension, fiber breakage continues until the length of the fiber fragment reaches a minimum dictated by the load carrying capability, or strength, of the fragment. This minimum length can be considered the "critical length" for this structure. The critical length has also been shown to decrease with increasing lateral pressure. Twist of the fiber and yarn diameter also play a role in determining critical length although it is thought that twist improves the strength of high-performance fibers but decreases the strength of low-performance fibers (6).

Based on statistical interpretation of experimental data, Pan (7) has proposed the following strength relationship.

$$\frac{\sigma_y}{\sigma_b} = \left(\frac{l_f}{l_c}\right)^{1/\beta} v_f\eta \tag{3}$$

where σ_y is the yarn strength, σ_b is the fiber bundle strength, l_f, l_c are the fiber length and critical length respectively, v_f is the volume fraction of packing density of the yarn, and β, η are the Weibull shape parameter and orientation efficiency factor respectively. An expression for the critical length of a yarn was presented by Realff (8)

$$l_c = \frac{2T_f}{\pi d \mu \sigma_l} \tag{4}$$

where, T_f is the fiber tensile force at yarn fracture, d is the yarn diameter, σ_l is the lateral pressure, and μ is a frictional coefficient.

Investigations by Gosh (9), (10) have demonstrated yarn mechanical behavior for a variety of material systems. Their studies have highlighted the influence of the helical geometry of the twisted yarn and the role of the resultant multiaxial forces generated during yarn axial tension by the unique structural arrangement of the fibers. Based upon test observations, they have proposed the following empirical expression for yarn tenacity, denoting the strength of a yarn of given linear density.

$$Q = \frac{n_h}{n_e} F_h \frac{\vartheta_b}{100} \cos^2 \theta \tag{5}$$

The terms of equation(5), defined below, are determined from test and observation. The concepts of yarn tenacity and the relationships to stress can be found in (11).

n_h = number of fibers at location of yarn break

n_e = average number of fibers in yarn cross-section

$n_h = n_e - 1.96\sigma$

σ = standard deviation for 95% confidence level of number of fibers in yarn cross-section

F_h = fiber bundle tenacity at gage length

θ = average helix angle of fibers in yarn failure zone

ϑ_b = percent of broken fibers in yarn failure zone

The basic unit of the yarn is the MWCNT. In order to investigate the deformation and forces on a bundle of nanotubes, molecular dynamics simulations were performed of a system of (10,10) single-walled carbon nanotubes. Each nanotube contained 880 carbon atoms per 5.425 nm length. The nanotubes were simulated in a periodic box which contained 9 nanotubes. Each nanotube was represented with the Brenner-Tersoff potential (12). The intra-nanotube interactions were modeled with the Lennard-Jones potential. The box was subjected to compression in the transverse x and y- directions. No change was made to the z-direction. The percent of deformation relative to the starting configuration is included in Table 1. Altogether, five levels of compression were simulated up to 15% compression. At each level of compression strain, two simulations were performed. The first was carried out under equilibrium NVE (constant Number of particles, constant Volume, and constant Energy) conditions and the normal force on one of the nanotubes was calculated in the direction normal to the nanotube surface. In the second simulation, the nanotube was loaded incrementally with axial force on each atom until the nanotube began to slide. Both the velocity of the

nanotube and the distance that it traveled were monitored throughout the simulation. Two definitions were used to determine the initiation of nanotube axial motion. In the first, the nanotube velocity was consistently positive above the thermally induced velocity fluctuations. In the second definition, the nanotube was considered to be moving when it had traveled for 0.2 nm. The friction coefficient is calculated as the negative of the ratio of the applied to the normal load and is presented in Table 2.

Table 1. Stress on the Nanotube System under Compression

Percent Compression (Nominal)	Stress Component in Transverse or x-direction (GPa)	Stress Component in Axial or z-direction (GPa)
0	-0.18±0.12[a]	-0.04±0.08
2	1.7± 0.2	0.80±0.11
5	1.8±0.3	0.97±0.14
10	1.9± 0.5	1.2±0.2
15	1.9±-0.3	1.64±0.14

[a]Deviations are for 1600 points on the trajectory spaced at 50 time steps apart.

Table 2. Apparent friction coefficient for nanotube sliding.

Percent Compression (Nominal)	Method of Determining Pull-Through Force	Pull-Through Force (pN/atom)	Normal Force (pN/atom)	Apparent Friction Coefficient
0	velocity	0.053[a]	-0.3±1.4[b]	--
	distance	0.065		--
2	velocity	0.120	-8.0±4	0.015±0.006[c]
	distance	0.120		0.014±0.006
5	velocity	0.075	-9.0±3	0.008±0.002
	distance	0.068		0.008±0.003
10	velocity	0.083	-5.0±3	0.015±0.009
	distance	0.081		0.015±0.010
15	velocity	0.043	-5.0±2	0.009±0.003
	distance	0.030		0.006±0.002

[a]Averaged from 2 simulations. No uncertainties reported.
[b]Deviations are the standard deviation of the mean for 80 values 1000 time steps apart.
[c]Deviation propagated from standard deviation of the mean in the normal force.

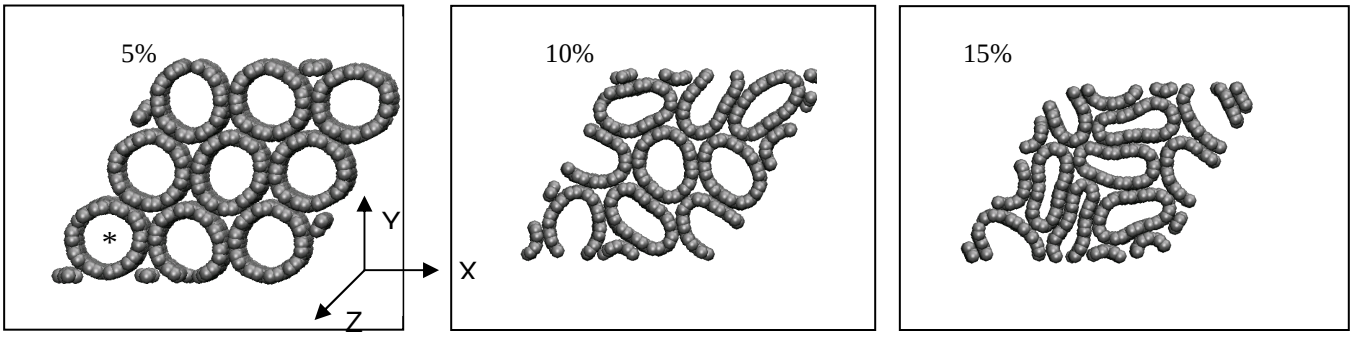

Figure 2. Illustration of increasing lateral compression on the deformation of a tube bundle.

The molecular structure of carbon nanotubes (Figure 2) is simulated with and without transverse compression. While the nanotube system is compressed, the relationship between the stress in the transverse direction and the normal load on the nanotube is non-linear. This non-linearity is expected when monitoring the nanotubes deformation under compression (Figure 2). The marked nanotube (*) in Figure 2 was loaded in the axial direction to simulate tube-tube interactions due to sliding of nanotubes relative to each other. Recall that the structures illustrated in Figure 2 are periodic in the simulation.

The calculated friction coefficient cannot be determined for the undeformed structure because the normal force is too close to zero. However, the compressed systems have friction coefficients which are on the same order of magnitude as is the normal force on the nanotube in the compressed systems. Relative to the undeformed system, the normal force on the nanotube is reduced. The pull-out force initially increases at 2% compression then reduces with increasing compression. It is expected that during scale-up to the macro-scale, the normal force on the nanotubes could be related to lateral forces induced under twist and axial load of a single yarn.

The frictional characteristics of nanotubes have been shown by two of the authors (13) to vary in different environments. For example, a study using a similar analysis of the frictional behavior of a nanotube sliding on a non-smooth surface of the inside of a functionalized outer nanotube showed different friction characteristics than when it slid on a smooth surface of the inside of a non-functionalized outer nanotube. When the outer nanotube is not functionalized, the inner one slips easily in the axial direction. Therefore, the nanotube has a low friction coefficient in the non-functionalized case. When the outer nanotube is functionalized, the (absolute value) magnitude of the normal force is much smaller than the non-functionalized case most likely because the roughening of the surface reduces the contact area with the inner nanotube, and the inner one ‘sticks’ while trying to move axially within the rough surface of the outer nanotube. Both of

these changes in the nanotube physical behavior work together to raise the nanotube friction coefficient in the functionalized systems relative to the non-functionalized systems. As demonstrated by others (14), additional changes to nanotube sliding behavior occurs when there are defects in the outer nanotube or covalent bonding between nanotubes in MWCNTs.

At the atomistic scale, MD simulations were used to estimate the load transferred to the central nanotube as a nanotube bundle of 9 nanotubes is twisted. The transferred load in the bundle, defined as the axial load that is passed on to the central tube in the bundle for a nanotube bundle with a specific degree of twist versus the twist angle, is calculated from 0-210 degrees. Based on this definition, at zero degrees a force of 0.048 eV/A is transferred, and at 120 degrees the transferred load peaks at 1.63 eV/A. The degree of twist of nanotubes at the nanoscale is expected to be small relative to the overall yarn twist. It is assumed that the controlling parameters are connected to the transverse compression effects in the fibers which in turn put pressure on the inner nanotubes. As described by Frankland (13), investigations of the composite should also consider covalent bonding of the nanotubes to the polymer.

The complex geometry associated with twist and material variations implies that the macro-scale modulus of a yarn is a volume averaged structural property rather than a material property. This complexity results in geometry and axial load affecting all the mechanical properties of a twisted yarn. During tensile loading of the yarn, the apparent stress-strain behavior will generally have a short linear region characterized by slippage of the fibers followed by nonlinearity with considerable extension while the fibers continue to slip, and finally fiber and yarn failure occurs. During this axial loading of the yarn, off-angle forces in the yarn are generated by yarn twist. This multiaxial load state consists of combinations of axial tension and lateral compression.

Test Methods

During tensile loading, the composite reveals yarn stress-strain behavior similar to the stress-strain behavior of a single fiber. The five-yarn polymer composite used in this study was subjected to uniaxial tension, at room temperature, in a pneumatic test stand with load measured using a standard load cell calibrated to +/-10N. The stress reported is engineering stress, based on the load cell data and the average specimen cross-sectional area in the gage section. The static tests are conducted with a small tensile preload and a constant displacement rate of 17mm/min for all the specimens. Once loaded to 50% of the gage length, the sample is unloaded at the same rate. Axial strain is calculated as the change in grip or crosshead displacement divided by the initial crosshead displacement as measured by the test machine's displacement transducer. Additional information on test procedures can be found in a recent publication by the authors (15).

A portion of the polymer and composite specimens were exposed to 75% relative humidity (RH) and 75^{o}C (hot/wet) for periods up to 60 days to allow initial assessment of the effects of environmental conditioning. During conditioning, mass change of each specimen was measured (Figure 3).

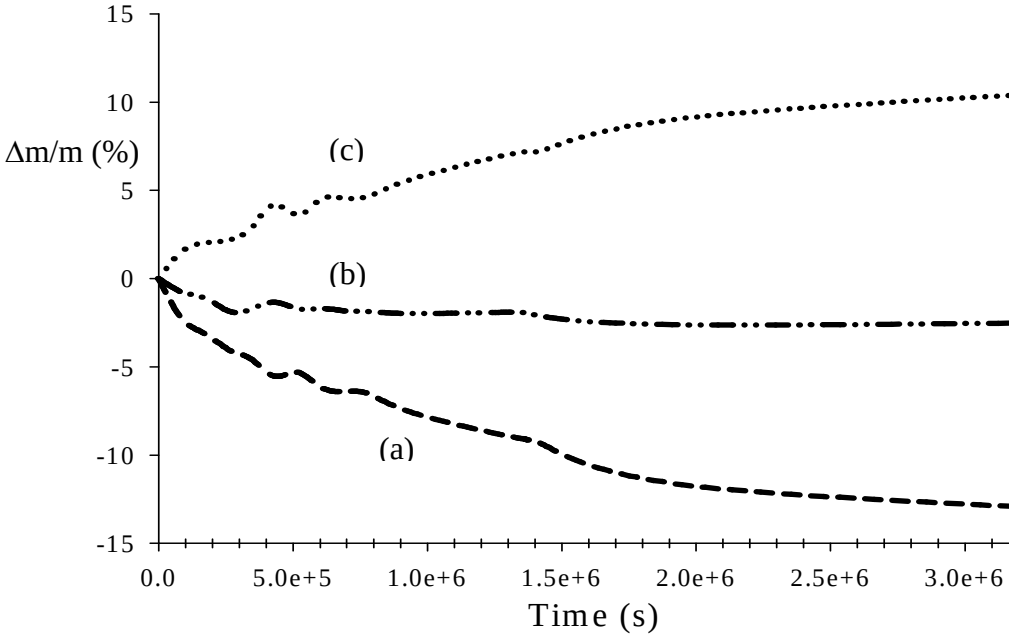

Figure 3. Measured mass change in polymer and composite samples after aging at 75°C and 75% RH.

Curves (a) and (b) on Figure 3 represent an average response of at least 3 individual specimens. Curves (a) and (b) illustrate a mass loss increasing with time for the polymer and composite samples respectively. Curve (c) illustrates the difference between (a) and (b) and is assumed to represent a mass increase in the "yarns." It is inferred then, that for this system, aging has resulted in degradation of the polymer and moisture absorption by the MWCNT yarns.

Periodic measurements of the dynamic mechanical response using standard dynamic mechanical analysis (DMA) equipment were made to assess physical changes in the material system. Representative stress-strain data from the DMA tests are given in Figure 4 for the baseline 5-yarn composite (unaged). The specimens were cycled 50 times under force control at 1Hz. After the first few cycles, the response remains relatively unchanged over the course of remaining cycles.

Stress-strain curves from the static tensile tests (polymer and composite) were influenced by the hot/wet aging. Figure 5 contains five different curves, each one representing a change in material or a change in aging condition. An explanation of the five curves is provided in the caption of Figure 5. In general, it was found that aging of the polymer decreases stiffness and initial failure strength for both the polymer and the composite.

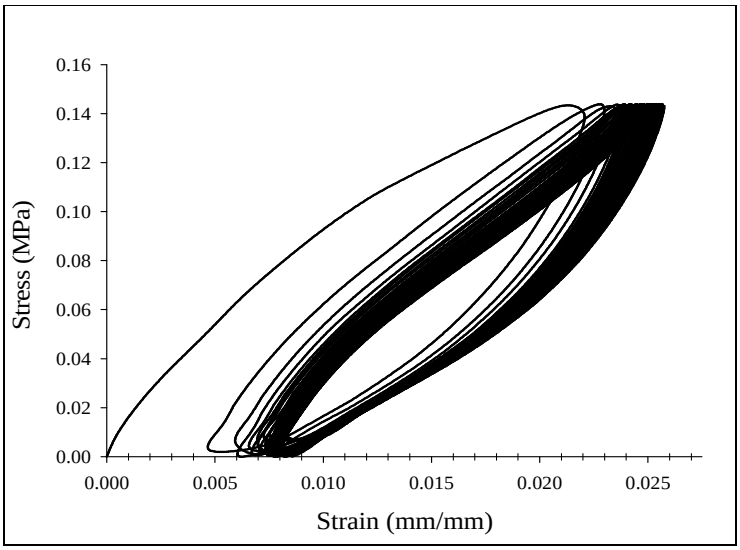

Figure 4. Representative stress-strain (DMA) for an unaged, 5 yarn composite.

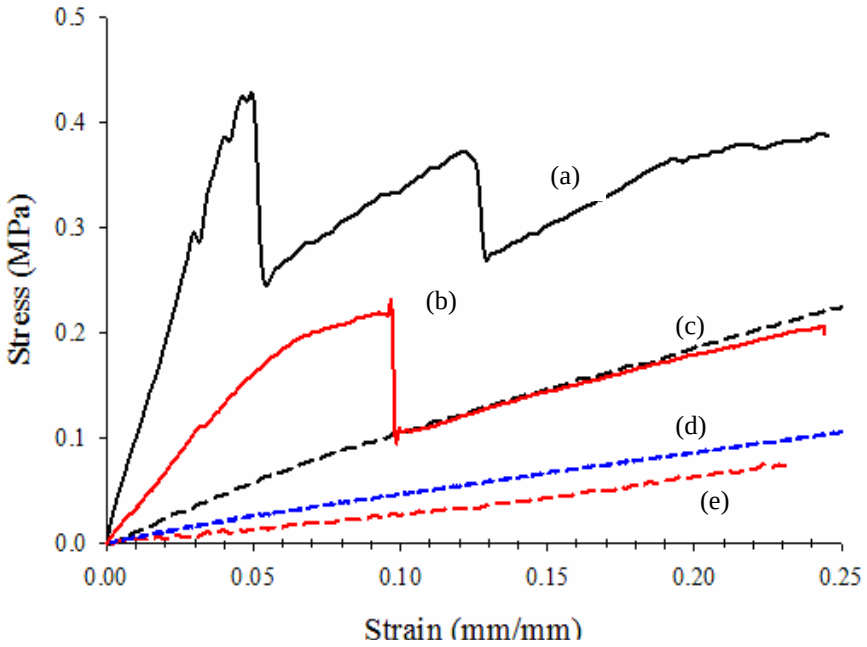

Figure 5. Representative stress strain curves from static tensile tests. Curve (a) is the 5 yarn composite baseline (unaged), Curve (b) is the 5 yarn composite after aging at 75°C/75% RH; Curve (c) is the polymer baseline (unaged); Curve (d) is the polymer after aging at RT/100% RH; Curve (e) is the polymer after aging at 75°C/75% RH.

The failure process in the MWCNT yarns embedded in a compliant polymer matrix can be complex and dependent upon both geometric and material parameters. In order to illustrate the progressive failure observed in the composite, a representative room temperature, stress-strain curve for the static tensile test of

the unaged 5-yarn composite is provided in Figure 6. Referring to this figure, upon loading, an elastic range can be defined (point 1). Maximum stress (points 2 and 3) correspond to initial failure. Video evidence suggests, at initial failure, all five yarns failed simultaneously at the same location with respect to the longitudinal axis. The majority of test specimens had initial failure occur in the gage section. Upon further loading, the specimen has lost stiffness (point 4) but continues to carry load until the stress reaches the secondary failure level (point 5). At this point simultaneous failure of all five yarns occurs again but at a location different from the point of initial failure. During loading, the yarn fails progressively in distinct segments, and the effective stiffness of the composite tends toward the stiffness of the polymer matrix (point 6). This failure mode is depicted in a photograph (Figure 7) for a typical failed composite. Upon unloading (point 7), the specimen does not return to its initial strain value (point 8).

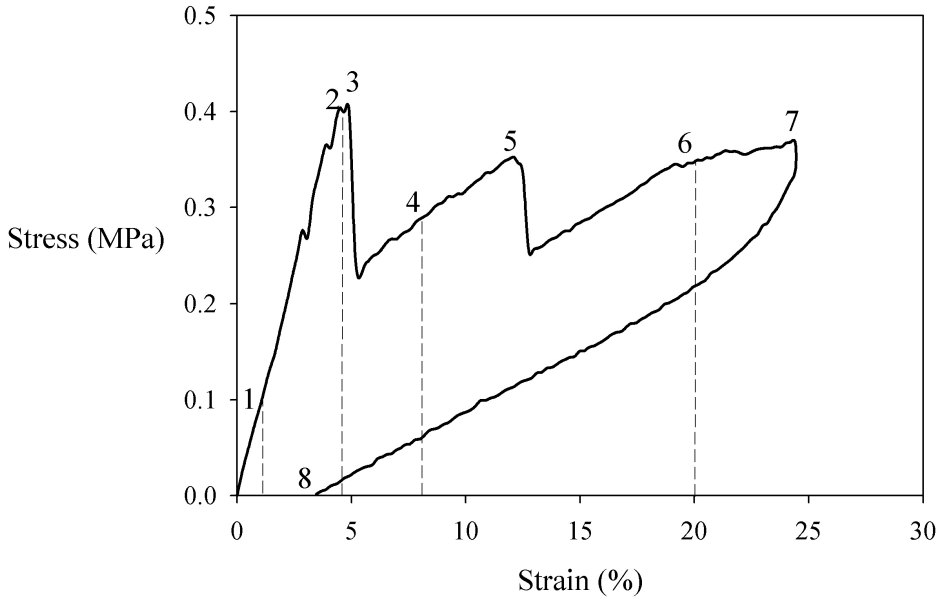

Figure 6. Representative Engineering Stress - Strain curve for 5 yarn composite loaded in static tension. Note: 1 – 1% strain; 2 – 4.5% strain; 3 – first failure across all yarn; 4 – 8% strain; 5 – secondary failure; 6 – 20% strain; 7 – 50% gage length (point of unload); 8 – final strain

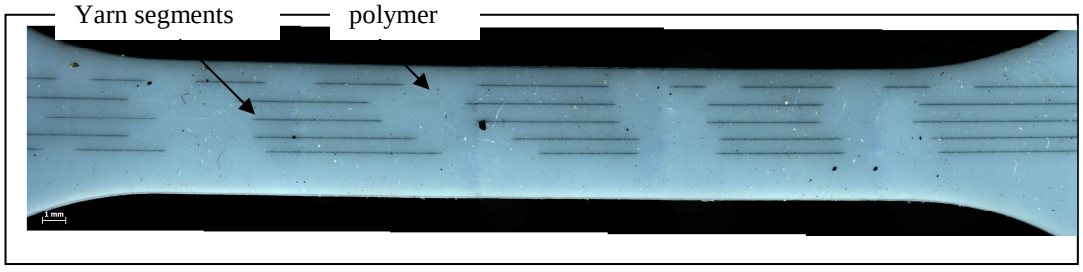

Figure 7. Optical microphotograph (12x) of failed composite tensile specimen illustrating the sequence of yarn segments.

Despite the low yarn volume fraction, the composite modulus was increased by over a factor of ten compared to the base polymer. The composite exhibited linear elastic behavior up to initial failure. The high strain value (~5%) reached in the test resulted in catastrophic yarn failure with all yarns failing simultaneously at some characteristic length. Failure modes of the yarns were not unlike fabric yarn failure modes described in the textile literature. As is typical with twisted yarns, the final yarn structure or bundle does not retain the strength or stiffness of the base material or strands.

Summary and Results

A parametric study has been performed on multi-walled carbon nanotube spun yarns using analysis tools and laboratory test data. Key structure-property relationships were defined at the macro-scale using textile mechanics. Twist and friction for bundles of carbon nanotubes were explored at the nano-scale using atomistic simulations. The behavior of the base polymer was compared to a low volume fraction, unidirectional, composite that was made of compliant polymer and five, four-ply yarns spun from a forest of multi-walled carbon nanotubes. The influence of aging specimens at hot/wet conditions was evaluated by mass changes over time and residual mechanical properties.

The results provided insights into the relative influence of parameters such as yarn twist angle, yarn volume fraction, and nanotube-to-nanotube interactions including friction developed by twist and mechanical loading. Deformation, failure modes and failure mechanisms of the yarn structure were found to closely resemble the well-documented behavior of standard textile yarns. The dominant failure mode under tension was the formation of increasingly shorter yarn segments whose ability to carry load was diminished as the segments approached some critical length. Careful examination of the failed yarns indicates that the dominant failure mechanism was the yarn unraveling leading to segmentation. Elastic spring-back of the failed yarn segments also was observed.

Aging of the polymer and the composite using aggressive hot/wet conditions reduced the stiffness of the material systems. A study in mass change at specific aging intervals indicates that the yarns may be capable of increasing mass due to water uptake. Although the stress-strain response and failure characteristics of the aged composite had the same general form as the unaged system, the here is a need for a broader test program before specific conclusions can be reached.

The use of well-defined nano-structured materials, such as carbon nanotubes, for the precursor for the spun yarn, will require multiscale analytical methods. The insights on tube-tube interactions and the possibilities of quantifying the influence of specific parameters, such as friction and the relationships to twist and load, illustrate the need for nano-scale modeling using molecular dynamics or other atomistic methods. At the macro-scale, standard textile mechanics can be used with some confidence for analysis and definition of key structure-property relationships necessary for aiding in the design of novel materials. It should be noted that a yarn is a structure, not a material, and as such each new variation of yarn design will produce a different set of properties. However, the analysis and test methods outlined in this paper are general enough to be considered for any number or combination of yarn structures and precursor materials.

References

[1] M. Zhang, Atkinson, K.R., and Baughman, R.H., "Multifunctional Carbon Nanotube Yarns by Downsizing an Ancient Technology," *Science*, 2004, 306: pp. 1358-1361.

[2] A.B. Dalton, et al., "Super-tough carbon-nanotube fibres," *Nature*, 2003, 423 (723).

[3] M. Zhang, et al., "Strong, Transparent, Multifunctional, Carbon Nanotube Sheets," *Science*, 2005, 309(1215): pp. 1215-1219.

[4] A. Bogdanovich, et al. "Fabrication and Mechanical Characterization of Carbon Nanotube Yarns, 3-D Braids, and their Composites," in *SAMPE Fall Technical Conference*. 2006, Dallas, TX.

[5] J.W.S. Hearle, *Yarn Texturing Technology*, ed. W.P. Limited. 2000, Cambridge.

[6] Y. Rao and Farris, R.J., "A Modeling and Experimental Study of the Influence of Twist on the Mechanical Properties of High-Performance Fiber Yarns," *Journal of Applied Polymer Science*, 2000, 77: pp. 1938-1949.

[7] N. Pan and Hua, T., "Relationship Between Fiber and Yarn Strength," *Textile Research Journal*, 2001, 71(11): pp. 960-964.

[8] M.L. Realff, et al., "A Stochastic Simulation of the Failure Process and Ultimate Strength of Blended Continuous Yarns," *Textile Research Journal*, 2000, 70(5): pp. 415-430.

[9] A. Ghosh, Ishtiaque, S.M., and Rengasamy, R.S., "Analysis of Spun Yarn Failure, Part I: Tensile Failure of Yarns as a Function of Structure and Testing Parameters," *Textile Research Journal*, 2005, 75(10): pp. 731-740.

[10] A. Ghosh, Ishtiaque, S.M., and Rengasamy, R.S., "Analysis of Spun Yarn Failure, Part II: The Translation of Strength from the Fiber Bundle to Different Spun Yarns," *Textile Research Journal*, 2005, 75(10): pp. 741-744.

[11] J.W.S. Hearle, Grosberg, P., and Backer, S., *Structural Mechanics of Fibers, Yarns, and Fabrics*. Vol. 1. 1969, New York: Wiley-Interscience.

[12] D.W. Brenner, "Empirical Potential for Hydrocarbons for use in Simulating the Chemical Vapor Deposition of Diamond Films," *Physical Review B*, 1990, 42: pp. 9458-9471.

[13] S.J.V. Frankland, Odegard, G.M., and Gates, T.S. "The Effect of Functionalization on Double-Walled Nanotube Materials," in *International Symposium on Clusters and Nano-Assemblies: Physical and Biological Systems*. 2003, Richmond, VA.

[14] M.F. Yu, et al., "Strength and breaking mechanism of multiwalled carbon nanotubes under tensile load," *Science*, 2000, 287: pp. 637-640.

[15] G.D. Jefferson, Gates, T.S., and Kahng, S. "Mechanical Performance of Multiscale Multi-wall Carbon Nanotube Twisted Yarns," in *SAMPE Annual Technical Conference*. 2007, Cincinnati, OH.